2016

Toolbox for Exploring Modular Gene Regulation in Synthetic Biology Training

Michael S. Magaraci
University of Pennsylvania, magaraci@seas.upenn.edu

Jessica G. Bermudez
University of Pennsylvania

Deeksha Yogish
University of Pennsylvania

Daniel H. Pak
University of Pennsylvania, pakdan@seas.upenn.edu

Viktor Mollov
University of Pennsylvania

See next page for additional authors

Recommended Citation

Magaraci, M. S., Bermudez, J. G., Yogish, D., Pak, D. H., Mollov, V., Tycko, J., Issadore, D., Mannickarottu, S. G., & Chow, B. Y. (2016). Toolbox for Exploring Modular Gene Regulation in Synthetic Biology Training. *ACS Synthetic Biology,* http://dx.doi.org/10.1021/acssynbio.6b00057

Toolbox for Exploring Modular Gene Regulation in Synthetic Biology Training

Abstract
We report a toolbox for exploring the modular tuning of genetic circuits, which has been specifically optimized for widespread deployment in STEM environments through a combination of bacterial strain engineering and distributable hardware development. The transfer functions of 16 genetic switches, programmed to express a GFP reporter under the regulation of the (acyl-homoserine lactone) AHL-sensitive luxR transcriptional activator, can be parametrically tuned by adjusting high/low degrees of transcriptional, translational, and post-translational processing. Strains were optimized to facilitate daily large-scale preparation and reliable performance at room temperature in order to eliminate the need for temperature controlled apparatuses, which are both cost-limiting and space-constraining. The custom-designed, automated, and web-enabled fluorescence documentation system allows time-lapse imaging of AHL-induced GFP expression on bacterial plates with real-time remote data access, thereby requiring trainees to only be present for experimental setup. When coupled with mathematical models in agreement with empirical data, this toolbox expands the scalability and scope of reliable synthetic biology experiments for STEM training.

Keywords
STEM, quorum sensing, LuxR, hardware

Disciplines
Biomedical Engineering and Bioengineering | Engineering

Author(s)
Michael S. Magaraci, Jessica G. Bermudez, Deeksha Yogish, Daniel H. Pak, Viktor Mollov, Josh Tycko, David Issadore, Sevile G. Mannickarottu, and Brian Y. Chow

Toolbox for Exploring Modular Gene Regulation in Synthetic Biology Training

Michael S. Magaraci, Jessica G. Bermudez, Deeksha Yogish, Daniel H. Pak, Viktor Mollov, Josh Tycko, David Issadore, Sevile G. Mannickarottu, and Brian Y. Chow*

Department of Bioengineering, University of Pennsylvania, Philadelphia, Pennsylvania 19104, United States

* Email: bchow@seas.upenn.edu, 215-898-5159

Abstract:

We report a toolbox for exploring the modular tuning of genetic circuits, which has been specifically optimized for widespread deployment in STEM environments through a combination of bacterial strain engineering and distributable hardware development. The transfer functions of 16 genetic switches, programmed to express a GFP reporter under the regulation of the (acyl-homoserine lactone) AHL-sensitive luxR transcriptional activator, can be parametrically tuned by adjusting high/low degrees of transcriptional, translational, and post-translational processing. Strains were optimized to facilitate daily large-scale preparation and reliable performance at room temperature in order to eliminate the need for temperature controlled apparatuses, which are both cost-limiting and space-constraining. The custom-designed, automated, and web-enabled fluorescence documentation system allows time-lapse imaging of AHL-induced GFP expression on bacterial plates with real-time remote data access, thereby requiring trainees to only be present for experimental setup. When coupled with mathematical models in agreement with empirical data, this toolbox expands the scalability and scope of reliable synthetic biology experiments for STEM training.

Keywords: STEM, quorum sensing, LuxR, hardware

Introduction

Synthetic biology experiments are powerful vehicles for inspiring interest in STEM fields, teaching critical concepts in gene regulation and cellular physiology, and applying engineering frameworks to biological problems through combined experimentation and mathematical modeling. [1-4] However, quantitative cell biology experiments are difficult to implement in training settings, due to (i) limitations in cost, equipment, space, and personnel, which are especially problematic for large group sizes, (ii) incompatibility of student academic schedules and extended laboratory access with the inherent time-courses of cellular phenomenon and well established laboratory protocols designed for research as opposed to scientific training, and (iii) poor experimental robustness against student inexperience with nuanced laboratory techniques, which can be particularly problematic if experiments must build on prior successful results. These practical challenges impede the implementation of hands-on laboratory practice coupled to mathematical modeling in mutually informative wet and dry laboratories.

Here, we report the creation of a toolbox to overcome the deployment challenges of synthetic biology experiments in STEM training laboratories, through a combination of bacterial strain engineering, protocol optimization, and hardware development. We engineered a genetic circuit based on the *Vibrio fischeri* quorum sensing (QS) system frequently studied to explore the principles of cell-cell communication, population dynamics, and the modular nature of genetic regulation. [2, 5-8] A set of 16 strains allows for the parametric tuning of the genetic transfer function through combinations of high/low levels of transcription, translation, inducer sensitivity, and post-translational degradation (schematized in **Figure 1a-c**). The strains were optimized to facilitate large-scale preparations and reliable room temperature growth in order to circumvent cost- and space-constraining temperature control systems that limit scalability. A distributable data acquisition system enables automated time-lapse imaging (and real-time data access) of GFP

reporter expression on bacterial plates over several days, thereby decoupling the scheduling of experiment setup from the continuous measurements needed to study nonsteady state and lengthy responses. Experimental results were in reasonable agreement with corresponding mathematical models for data reported here (as well as models and data generated by >120 undergraduates in the past two years). This infrastructure will enhance hands-on exploration of key gene regulation principles in synthetic biology and bioengineering.

Results and Discussion

Modular "Receiver" circuits[2, 5] report gene expression under the regulatory control of the luxR activator that is switched-on by a diffusible chemical signal (acyl-homoserine lactone, AHL). A constitutive promoter drives expression of luxR, which dimerizes upon binding of AHL and binds to its cognate pLux promoter to activate expression of the green fluorescent protein (GFP) reporter. The AHL-to-GFP transfer function or response curve is tunable at multiple levels of regulation in the suite of strains, which vary in (i) *E. coli* promoter strength driving constitutive luxR expression, (ii) AHL-to-luxR binding affinity, (iii) the strength of the ribosome binding site (RBS) preceding the GFP reporter, and (iv) presence/absence of a post-translational degradation tag (**Figure 1a-c**). Specifically, promoters were derived from the Anderson promoter collection[9] (strong, BBa_J23100; weak, BBa_J23109). AHL-to-luxR affinity was varied using the wild-type *Vibrio fisheri* gene and a hypersentive mutant, luxR-G2F.[10] RBS strength responsible for GFP translation was varied in the conservation of the Shine-Dalgarno sequence (BBa_B0034 and BBa_B0033 in the Registry of Standard Biological Parts [11, 12]). Finally, GFP degradation rate was varied through the addition of the LVA-ssrA degradation tag for clpX-mediated proteolysis. [13-16] To enhance scale-up, we chose NEB Turbo as the cellular chassis because the rapidly growing strain of *E. coli* decreases the time required for daily large-scale preparations to be manageable by a single person. Moreover, the use of NEB Turbo facilitates faster room temperature growth

during liquid culture and plate experiments in the absence of temperature control (protocols for large-scale sample preparation are provided in **Supporting Document 1;** Strain growth rate curves are provided in **Supporting Figure 1**).

Tuning the AHL response curve at the different aforementioned regulatory stages can be explored with a set of five strains, including a common "baseline" strain (**Figures 1c-e**). Strains programmed by all pairwise combinations of the tunable factors were also characterized (**Supporting Figures 2** and **3**). After 20 h room temperature growth, AHL response curves are readily measured on a plate reader, and strains with high GFP expression levels (i.e., greater than the baseline strain in black in **Figure 1**) are easily quantified on educational grade spectrophotometers (e.g., Ocean Optics Red Tide / Vernier). Even though the efficiency of the LVA tag is diminished at room temperature, [16] its effects are still highly detectable. A mathematical model adapted from Hill-based gene expression models[17, 18] reasonably captures the circuit-dependent transfer function characteristics (**Figure 1f,** see Materials and Methods for model). Experimental deviations from the modeled behavior primarily arise because a first-order luxR-concentration dependent term does not fully capture the effects of pLuxR leakiness. However, the first-order term was implemented for pedagogical simplicity because it still captures the salient features of promoter leakiness.

LuxR is highly studied in synthetic biology for its application to quorum sensing models. To facilitate the exploration of the spatiotemporal patterning of gene expression, we optimized the preparation and imaging of "Sender-Receiver" [5, 19] experiments, in which reporter expression in the Receiver is induced on bacterial plates by AHL which diffuses isotropically from a soaked filter disc that emulates a spatially localized ligand source in cell-cell signaling (**Figure 2a**). To minimize sample volume during autoclave preparation, a thin layer of cells in agarose was uniformly coated on top of the M9 minimal media plate, rather than embedded in the agar. [5]

To further address the incompatibility between student training schedules and extended gene expression time-course experiments, we developed a deployable (<$250), fully automated, and web-enabled fluorescence imager for remote data acquisition in bacterial plate experiments (**Figure 2b**). A laser-cut base houses blue LED strips for excitation. A custom Python script coordinates LED illumination and imaging of the plate(s) through a camera-equipped Raspberry Pi, which is mounted on a laser-cut hood. Plate images are stored locally on the Raspberry Pi and also pushed to a cloud server (in this case, Google Drive) for real-time remote access. This apparatus decouples experimental time at the bench from continuous time-course imaging over several days. The spatial gene expression patterning data, here also obtained at room temperature to circumvent incubators, agrees with mathematical models (**Figure 2c**,**d**) that combine numerical approximations for the nonsteady transfer functions and 2D diffusion. These models are appropriate for advanced undergraduate training (see Materials and Methods). For best results, we suggest using a strain with high expression levels (e.g., BC-A1-001 in **Supporting Figure 2**; represented as the gold strain in **Figure 1** and **Supporting Figure 3**). All CAD files, assembly instructions and schematics, and code are open source (**Supporting Document 2** and **Supporting File 1**).

Through focused strain development, protocol optimization, and hardware engineering, this toolbox was created to address issues of scaling in both size and scope, the latter of which can be adjusted from single-day demonstrations (e.g., spatial patterning of gene expression) to multiweek modules in which response curve measurements inform predictive modeling and experimental testing of the spatial patterning of gene expression (which we have successfully implemented in groups of 40-80 concurrent students on multiple occasions). It is a valuable addition to a growing community-wide infrastructure that includes training modules in light-gated gene expression ("Bactograph" [20,21]), the canonical *lac* operon and enzymatic synthesis of fragrant

compounds ("Biobuilder" [3, 4]), and accessible instrumentation (e.g., 3D-printed turbidostat [22]), all of which share a common goal for enhancing access to synthetic biology.

Materials and Methods

Strain Construction: Plasmid information is summarized in Supporting Figure 1. Plasmids were constructed via multipart Gibson Assembly using the high-copy pSB1C3 backbone vector.

Transfer Functions in Liquid Culture: Strains were grown overnight in LB media with 34 µg/mL chloramphenicol and then diluted 1:100 into M9 minimal media (with 34 µg/mL chloramphenicol, 1 mM thiamine hydrochloride, and 0.2% casamino acids). Cultures were grown at 37°C to reach mid-log phase and then diluted to $OD_{600} \approx 0.3$ for uniformity before AHL induction (Sigma-Aldrich K3007, < 1% v:v DMSO in all solutions). After 20 h growth at room temperature, OD_{600} and GFP fluorescence (excitation, 466 nm; emission: 511 nm) were measured on a Tecan Infinite m200 plate reader.

Spatial Patterning of Gene Expression on Plates: Strains were prepared as described above prior to induction. A 2 mL sample of culture ($OD_{600} \approx 0.3$) was diluted into 2 mL of 0.7% agarose (4 mL total) and then quickly poured over 100 mm M9-Chloramphenicol plates and allowed to dry. of AHL (10 µL of 1 µM, Figure 2) was placed on a sterile 5 mm filter paper disk (Sigma-Aldrich 74146, hole punched to correct size) and allowed to dry, after which the dry disk was centered on the bacterial plate.

Automated Imaging Acquisition: The automated imager was designed in Solidworks and laser-cut out of MDF. Strip LEDs (Oznium Super Thin Ribbon LED Strips) for illumination were controlled via a camera-equipped Raspberry Pi 2 Model B connected to a driver circuit (**Supporting Document 2**). The camera was focally adjusted (f=500 mm, Thorlabs LA1908-A), and controlled by a custom Python script that automatically pushes images to a cloud server (Google Drive) using the Drive linux library. All CAD files, drawings, parts list, Python code, Raspberry Pi configuration files, and support documentation can be found online (**Supporting Document 2** and **Supporting Files 1**; SD card image file with Raspberry Pi operating system and complete Solidworks Assembly files are hosted on the University of Pennsylvania Scholarly Commons).

Mathematical Modeling: A 3-equation system based on the Hill Function was adapted from a previous work[17] to model steady-state gene expression, where R = activated luxR (μM), ρ_R = formation rate of R (μM^{-3} min^{-1}), δ_R = degradation rate of R (min^{-1}), TX = GFP transcript (μM), α_{TX} = formation rate of TX (μM min^{-1}), δ_{TX} = degradation rate of TX (min^{-1}), K_R = luxR activation threshold (μM), n = Hill coefficient (dimensionless), β_{pluxR} = luxR promoter leakiness[23] (min^{-1}), α_{GFP} = formation rate of translated GFP (min^{-1}), δ_{GFP} = degradation rate of translated GFP (min^{-1}). All concentrations for molecular species should be in micromolar in order to prevent roundoff errors in MATLAB.

(1) $$\frac{d[R]}{dt} = (\rho_R[LuxR]^2[AHL]^2 - \delta_R[R])$$

(2) $$\frac{d[TX]}{dt} = \beta_{pluxR}[LuxR] + \left(\frac{\alpha_{TX}\left(\frac{[R]}{K_R}\right)^n}{1+\left(\frac{[R]}{K_R}\right)^n}\right) - \delta_{TX}\,[TX]$$

(3) $$\frac{d[GFP]}{dt} = (\alpha_{GFP}[TX] - \delta_{GFP}\,[GFP])$$

Nonsteady state gene expression was modeled using finite difference numerical approximations for eqs 1-3 (FTCS, forward time centered space approximations). Time-varying AHL profiles of 2D diffusion from the filter disc were modeled by FTCS approximations as previously reported, [5] and then passed into the dynamic gene expression model to solve for spatiotemporal patterning of GFP expression.

Supporting Information:

[Supporting Figure 1] Growth rate comparison of NEB Turbo and NEB 5α cells.

[Supporting Figure 2] Plasmid map and genetic circuit design summary.

[Supporting Figure 3] Transfer functions for 16 strains covering all pairwise combinations of individual parameters reported in Figure 1.

[Supporting Document 1] Large-scale sample preparation protocols for AHL response curve generation and spatial patterning of GFP expression on bacterial plates.

[Supporting Document 2] Automated imager assembly details, parts list, and Raspberry Pi automation setup.

[Supporting Files 1] Zip file containing CAD files for trans-illuminator and Python code for automation.

Author Contributions: M.S.M. and B.Y.C. designed all experiments, analyzed all data, and wrote the manuscript. M.S.M. conducted all experiments, with assistance from J.G.B. (all aspects), D.Y. (hardware), D.H.P. and V.M. (scale-up protocol development, reliability testing), and J.T. (model development). S.G.M. and D.I. assisted with training module development.

Acknowledgment: We thank Spencer Glantz and Shriram Sundararaman, as well as the NSF MSPES community (Multisite Public Engagement of Science in Synthetic Biology) for helpful discussion. This work was funded by the George H. Stephenson Foundation and the University of Pennsylvania Department of Bioengineering. M.S.M is supported by the NSF GRFP. B.Y.C. was supported by DARPA (HR0011-12-C-0068), NSF (CBET126497), NIH/NIDA (1R21DA040434-01), and the W.W. Smith Charitable Trust for the Heart. D.I. was supported by NIH/NCI (1R21CA182336-01A1).

REFERENCES:

[1] Endy, D. (2005) Foundations for engineering biology, *Nature 438*, 449-453.

[2] Canton, B., Labno, A., and Endy, D. (2008) Refinement and standardization of synthetic biological parts and devices, *Nat Biotech 26*, 787-793.

[3] Dixon, J., and Kuldell, N. (2011) BioBuilding using banana-scented bacteria to teach synthetic biology, *Methods Enzymol 497*, 255-271.

[4] Kuldell, N., Bernstein, R., Ingram, K., and Hart, K. M. (2015) *Biobuilder*, O'Reilly Media.

[5] Basu, S., Gerchman, Y., Collins, C. H., Arnold, F. H., and Weiss, R. (2005) A synthetic multicellular system for programmed pattern formation, *Nature 434*, 1130-1134.

[6] Haseltine, E. L., and Arnold, F. H. (2008) Implications of rewiring bacterial quorum sensing, *Applied and environmental microbiology 74*, 437-445.

[7] Dilanji, G. E., Langebrake, J. B., De Leenheer, P., and Hagen, S. J. (2012) Quorum Activation at a Distance: Spatiotemporal Patterns of Gene Regulation from Diffusion of an Autoinducer Signal, *Journal of the American Chemical Society 134*, 5618-5626.

[8] Carbonell-Ballestero, M., Duran-Nebreda, S., Montañez, R., Solé, R., Macía, J., and Rodríguez-Caso, C. (2014) A bottom-up characterization of transfer functions for synthetic biology designs: lessons from enzymology, *Nucleic Acids Research*.

[9] Andersen Promoter Collection - http://parts.igem.org/Promoters/Catalog/Anderson.

[10] Collins, C. H., Arnold, F. H., and Leadbetter, J. R. (2005) Directed evolution of Vibrio fischeri LuxR for increased sensitivity to a broad spectrum of acyl-homoserine lactones, *Mol Microbiol 55*, 712-723.

[11] Registry of Standard Biological Parts - http://parts.igem.org/Main_Page.

[12] Vilanova, C., and Porcar, M. (2014) iGEM 2.0 - refoundations for engineering biology, *Nat Biotech 32*, 420-424.

[13] Andersen, J. B., Sternberg, C., Poulsen, L. K., Bjorn, S. P., Givskov, M., and Molin, S. (1998) New unstable variants of green fluorescent protein for studies of transient gene expression in bacteria, *Appl Environ Microbiol 64*, 2240-2246.

[14] Karzai, A. W., Roche, E. D., and Sauer, R. T. (2000) The SsrA-SmpB system for protein tagging, directed degradation and ribosome rescue, *Nature structural biology 7*, 449-455.

[15] McGinness, K., Baker, T., and Sauer, R. (2006) Engineering controllable protein degradation, *Mol Cell 22*.

[16] Purcell, O., Grierson, C. S., Bernardo, M. d., and Savery, N. J. (2012) Temperature dependence of ssrA-tag mediated protein degradation, *Journal of Biological Engineering 6*, 1-3.

[17] Basu, S., Gerchman, Y., Collins, C. H., Arnold, F. H., and Weiss, R. (2005) A synthetic multicellular system for programmed pattern formation, *Nature 434*, 1130-1134.

[18] Basu, S., Mehreja, R., Thiberge, S., Chen, M. T., and Weiss, R. (2004) Spatiotemporal control of gene expression with pulse-generating networks, *Proc Natl Acad Sci U S A 101*, 6355-6360.

[19] Gerchman, Y., and Weiss, R. (2004) Teaching bacteria a new language, *Proceedings of the National Academy of Sciences of the United States of America 101*, 2221-2222.

[20] Levskaya, A., Chevalier, A. A., Tabor, J. J., Simpson, Z. B., Lavery, L. A., Levy, M., Davidson, E. A., Scouras, A., Ellington, A. D., Marcotte, E. M., and Voigt, C. A. (2005) Synthetic biology: engineering Escherichia coli to see light, *Nature 438*, 441-442.

[21] Bactograph - http://www.bactograph.org/index.html.

[22] Takahashi, C. N., Miller, A. W., Ekness, F., Dunham, M. J., and Klavins, E. (2015) A Low Cost, Customizable Turbidostat for Use in Synthetic Circuit Characterization, *ACS synthetic biology 4*, 32-38.

[23] Alon, U. (2016) *An Introduction to Systems Biology*, Chapman & Hall/CRC.

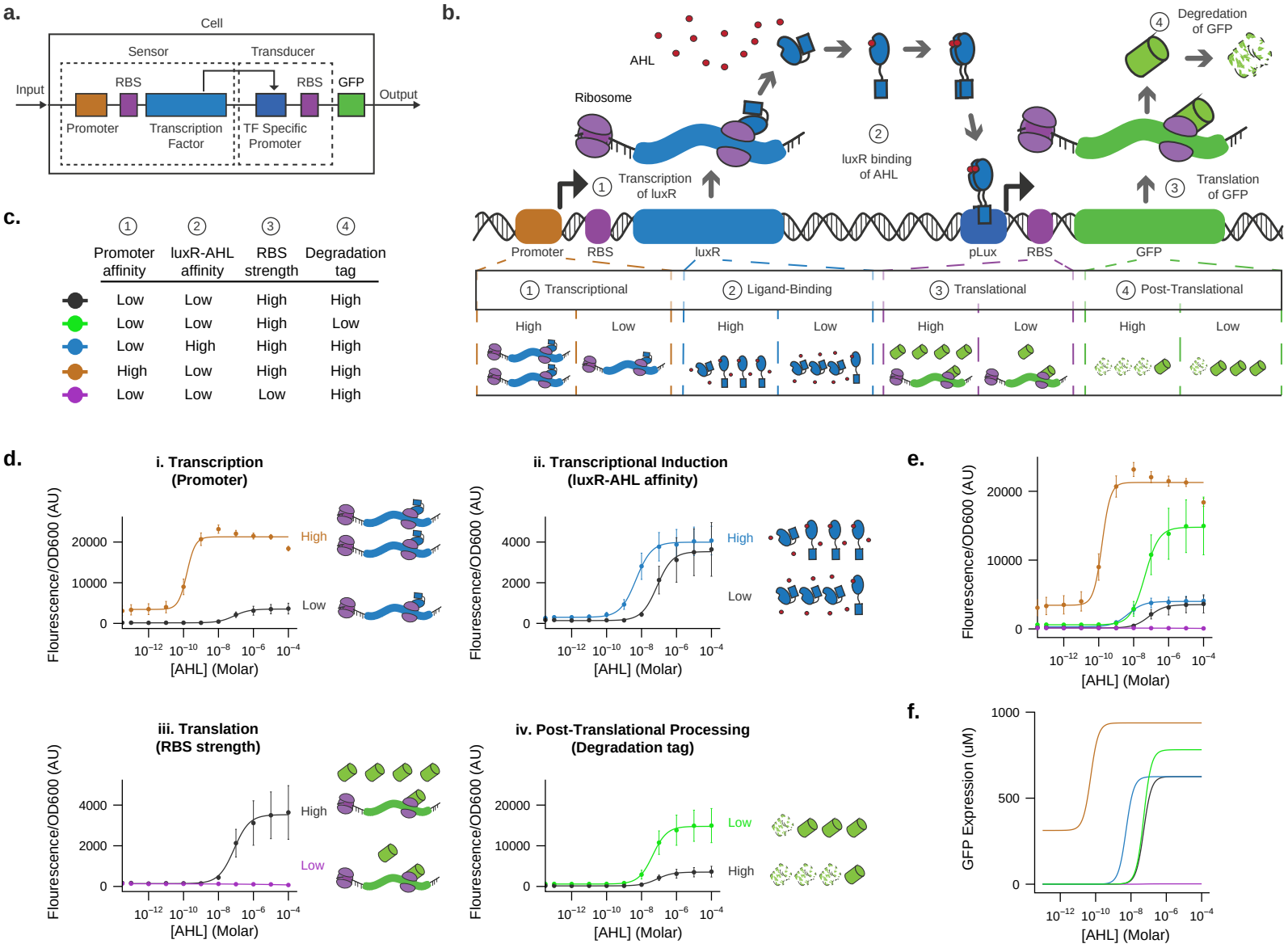

Figure 1. Parametric tuning of a genetic switch. (a) Simple genetic switch of a stimuli (input) responsive transcriptional activator that drives reporter protein expression (output) with a characteristic transfer function. **(b)** Engineered cell that expresses GFP under luxR transcriptional regulation in response to the acyl-homoserine lactone (AHL) ligand. The AHL-to-GFP response curve or transfer function of this "Receiver" circuit is tunable at multiple regulatory levels: (1) E. coli promoter strength (transcription), (2) luxR-AHL affinity (transcriptional induction), (3) RBS "strength" or Shine-Dalgarno sequence conservation (translation), and (4) LVA proteasomal degradation tag (post-translational processing). **(c)** Set of five bacterial strains for parametric tuning, engineered for room-temperature experiments to eliminate temperature control. **(d-f)** Transfer functions of strains with high/low parameter "strengths" vs. reference strain (black), taken 20 h postinduction and room temperature incubation **(d)** plotted individually by parameter or **(e)** altogether, are in reasonable agreement with **(f)** mathematical models. Error bars ± s.e.m.

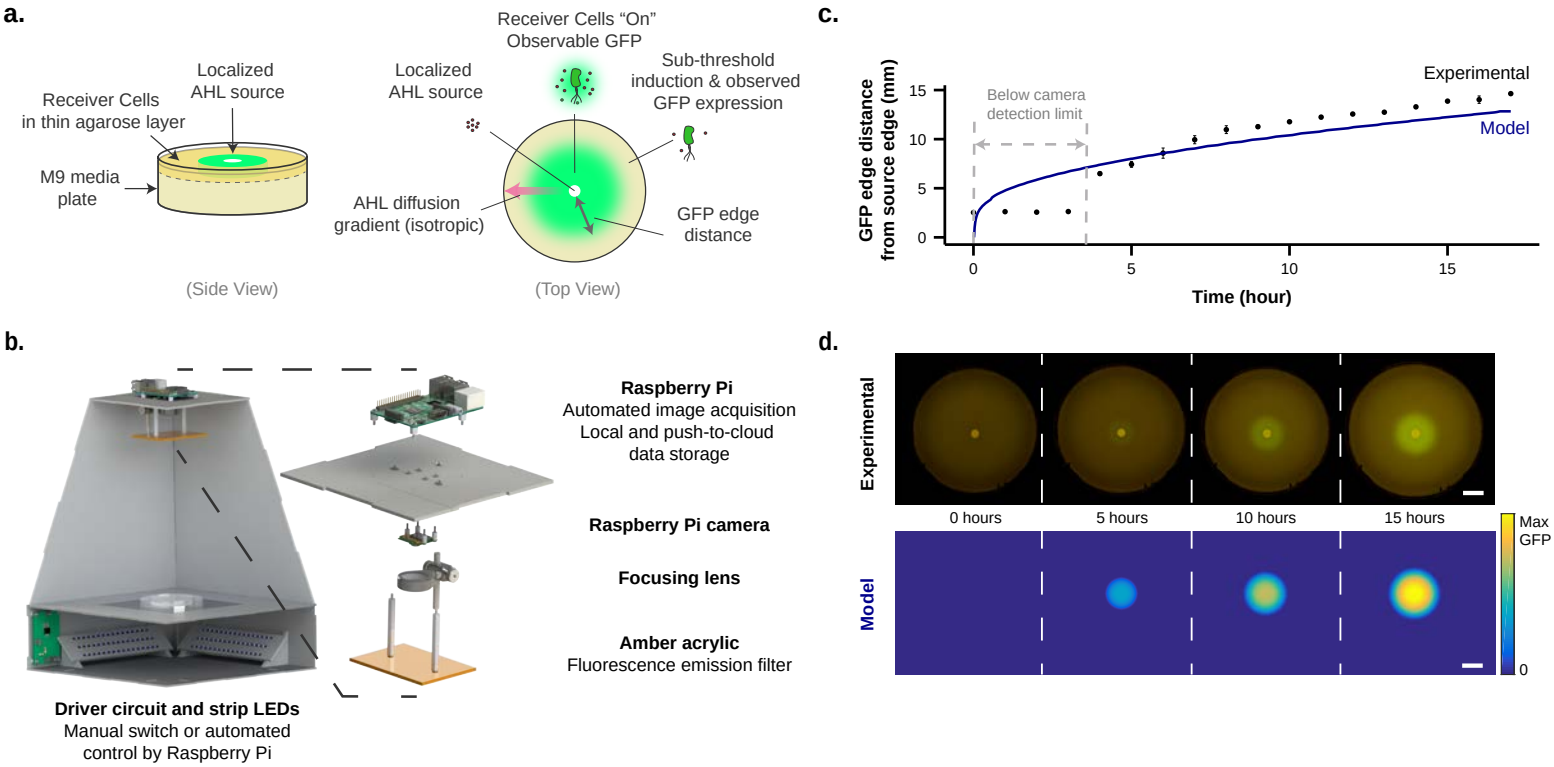

Figure 2. Spatiotemporal patterning of gene expression measured on an automated web-enabled fluorescence plate imager (a) GFP expression in a uniform film of plated Receiver cells is induced by AHL diffusing from a local source (filter paper), and results in a spreading edge of observed fluorescence. **(b)** Schematic of the accessible ($250) fluorescence plate imager, based on a Raspberry Pi camera module that automates data acquisition and pushes the data immediately to cloud storage for real-time remote access, which eliminates scheduling and laboratory access constraints in training environments. **(c)** Time course of observed GFP edge distance "spreading" (error bars ± s.e.m) is in agreement with a model that combines numerical approximations of diffusion and the AHL-to-GFP transfer function. **(d)** Representative images and heat maps from the model. Scale bar = 10mm. Experiments were conducted at room temperature.

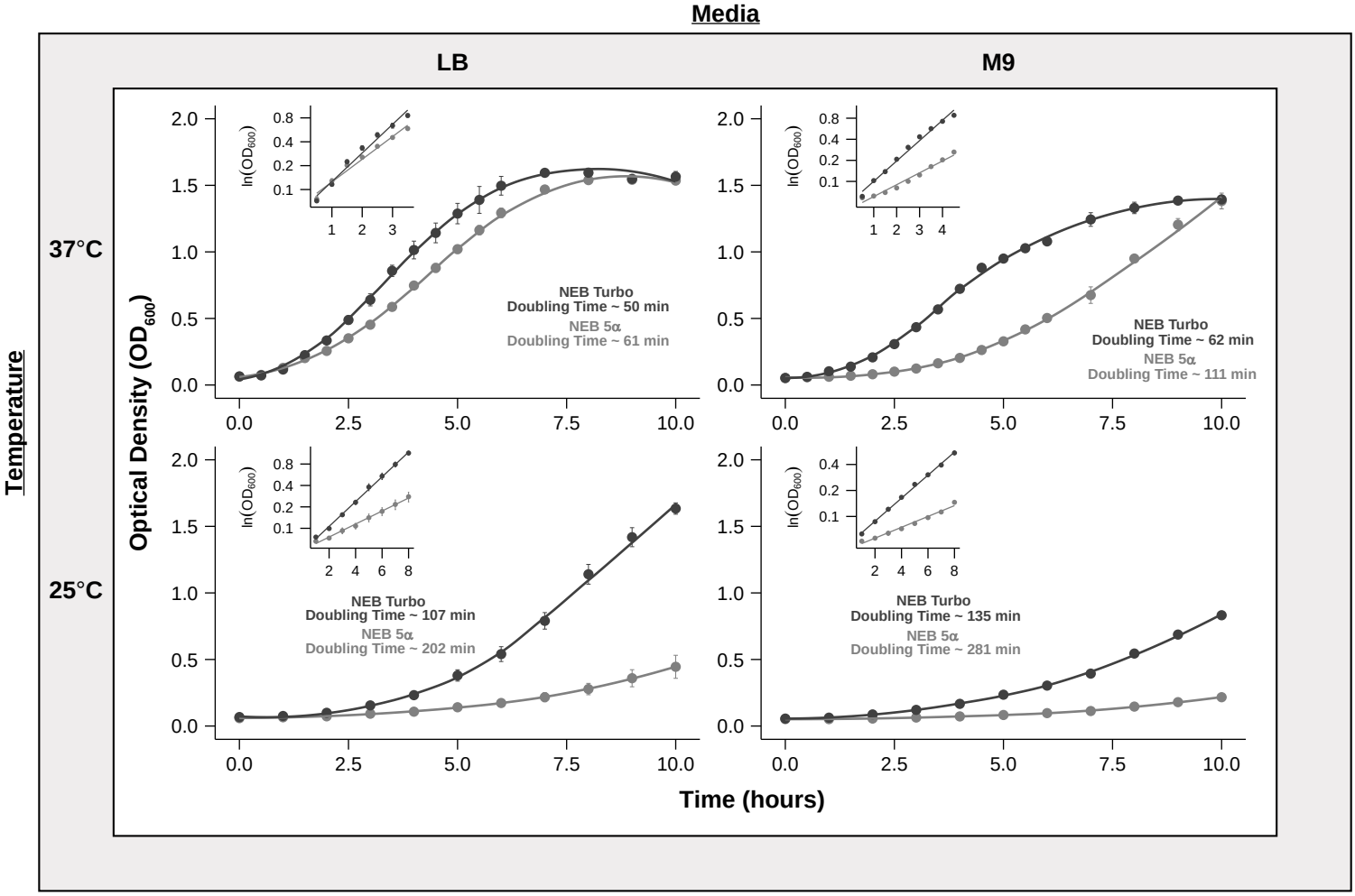

Supplementary Figure 1. Growth rate comparison between NEB Turbo and NEB 5α cells. Growth curves of NEB Turbo (dark gray) or NEB 5α (light gray) carrying plasmid BC-A1-001 in different media and temperature combinations. Overnight cultures were grown in LB media supplemented with 34 μg/mL chloramphenicol at 37°C and then diluted to OD600 = 0.05 in the experimental media (LB or M9). Cultures were transferred to an incubator at either 37°C or 25°C for the duration of the experiment. All growth curves were measured in triplicate and the data point represents the mean of three cultures. Error bars ± s.d. are smaller than the point size in some cases. Inset shows the exponential growth phase (log-transformed) used to calculate doubling time.

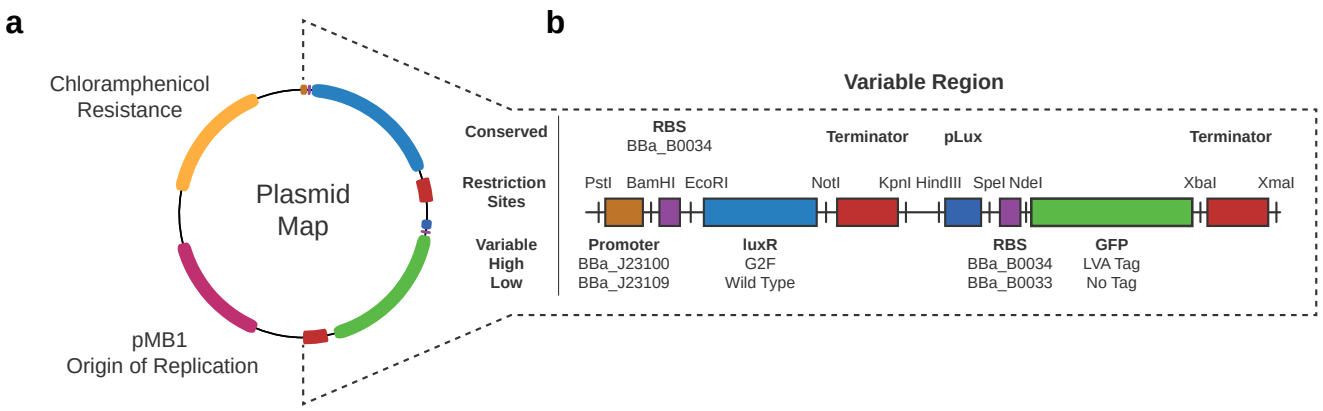

c

ID	Strain	Promoter	luxR	RBS	GFP
BC-A1-001	HLHH	BBa_J23100	Wild Type	BBa_B0034	LVA Tag
BC-A1-002	HLHL	BBa_J23100	Wild Type	BBa_B0034	No Tag
BC-A1-003	HLLH	BBa_J23100	Wild Type	BBa_B0033	LVA Tag
BC-A1-004	HLLL	BBa_J23100	Wild Type	BBa_B0033	No Tag
BC-A1-005	LLHH	BBa_J23109	Wild Type	BBa_B0034	LVA Tag
BC-A1-006	LLHL	BBa_J23109	Wild Type	BBa_B0034	No Tag
BC-A1-007	LLLH	BBa_J23109	Wild Type	BBa_B0033	LVA Tag
BC-A1-008	LLLL	BBa_J23109	Wild Type	BBa_B0033	No Tag
BC-A1-009	HHHH	BBa_J23100	G2F	BBa_B0034	LVA Tag
BC-A1-010	HHHL	BBa_J23100	G2F	BBa_B0034	No Tag
BC-A1-011	HHLH	BBa_J23100	G2F	BBa_B0033	LVA Tag
BC-A1-012	HHLL	BBa_J23100	G2F	BBa_B0033	No Tag
BC-A1-013	LHHH	BBa_J23109	G2F	BBa_B0034	LVA Tag
BC-A1-014	LHHL	BBa_J23109	G2F	BBa_B0034	No Tag
BC-A1-015	LHLH	BBa_J23109	G2F	BBa_B0033	LVA Tag
BC-A1-016	LHLL	BBa_J23109	G2F	BBa_B0033	No Tag

Supplementary Figure 2. Plasmid map and genetic circuit design summary. (a) Full plasmid map of the 16 genetic circuits constructed, with **(b)** the inset showing the variable region between all strains. **(c)** A table with all strain designations. Strain names follow the format of Promoter-luxR-RBS-GFP (H=High, L=Low, as defined in inset and Figure 1b).

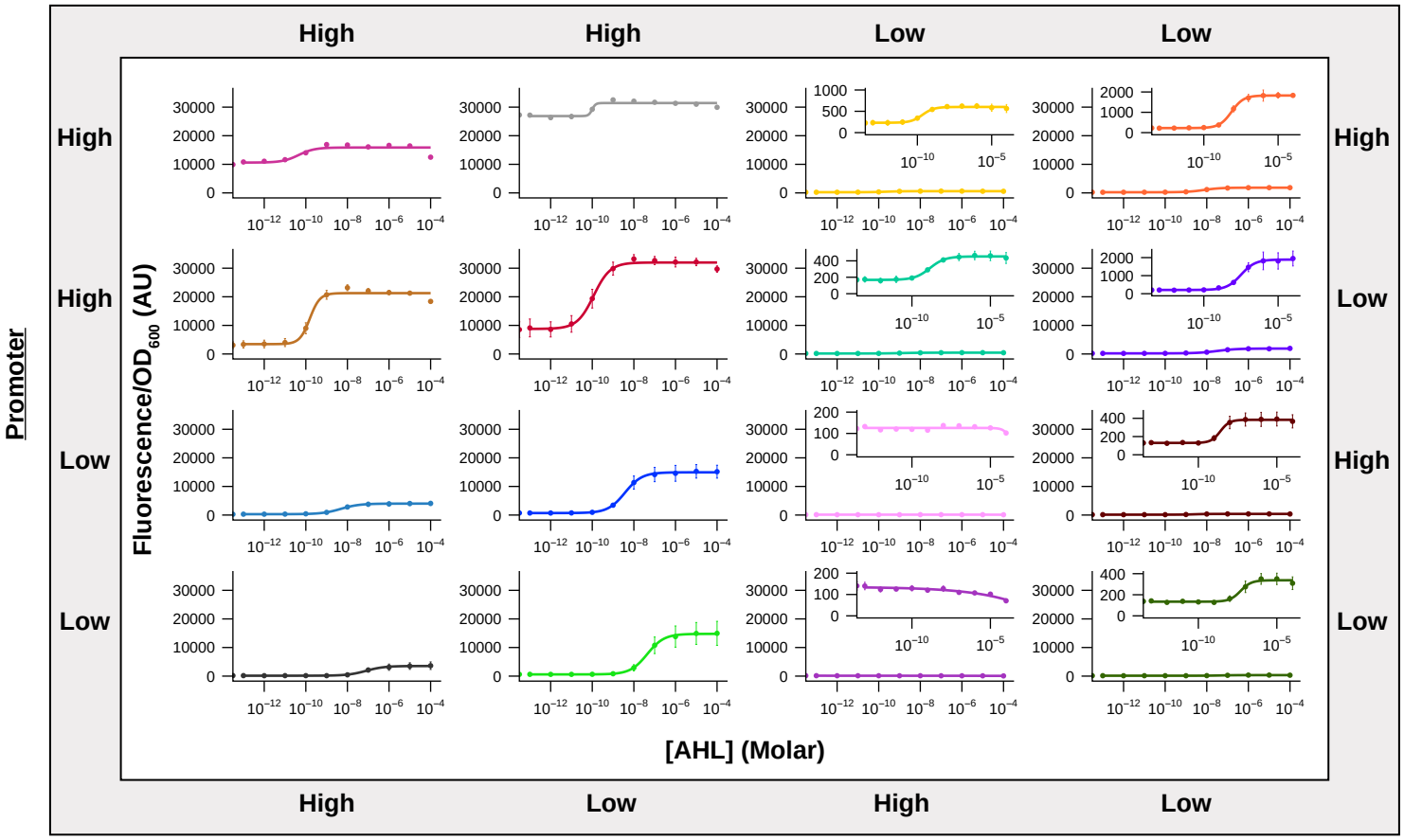

Supplementary Figure 3. Hierarchical tuning of "Receiver" cell transfer functions. AHL-to-GFP transfer functions of strains for all 16 pairwise combinations of individual parameters described in Figure 1b and Supplementary Figure 2c. Plots are displayed on the same scale to facilitate comparisons in relative expression levels and switching point concentrations, with inset boxes provided to resolve features. Error bars ± s.e.m are smaller than the point size in some cases.